Coordination Chemistry Reviews, *122* (1993) 91–107

Mathematical methods in coordination chemistry: topological and graph-theoretical ideas in the study of metal clusters and polyhedral isomerizations

R. Bruce King
Department of Chemistry, University of Georgia, Athens, GA 30602 (USA)

(Received 27 February 1992)

CONTENTS

A. INTRODUCTION

An area of increasing importance during the past several decades has been coordination chemistry, namely the chemistry of compounds containing central metal atoms surrounded by donor ligands of various types. Coordination compounds play major roles in diverse areas of practical importance ranging from molecular catalysis to solid state devices and metal ions in biological systems. The scientific and practical importance of coordination chemistry is indicated by large and regular international conferences on coordination chemistry since 1952.

One of my major research interests during the past two decades has been the development of new mathematical methods for understanding chemical structure, bonding, and reactivity, with particular emphasis on use of the mathematical disciplines of topology, graph theory, and group theory. This paper presents an overview of such work as applied to metal cluster bonding topology and polyhedral isomerizations, two areas of considerable interest to coordination chemists.

The idea for this paper originated from my lecture at a microsymposium that I organized at the 24th International Conference on Coordination Chemistry, which was held in Athens, Greece, in August, 1986. I have continued my activity in this area since that time. This paper presents a general view of some key ideas originating from this work. Readers wishing further details are directed to the cited references for additional information.

Correspondence to: R.B. King, Department of Chemistry, University of Georgia, Athens, GA 30602, USA.

0010-8545/93/$24.00

B. METAL CLUSTER BONDING TOPOLOGY

In 1977, King and Rouvray [1] first published a novel approach to metal cluster structure and bonding based on ideas taken from graph theory. Subsequent experience indicates the following strengths for this method:

(1) the ability to deduce important information about the electron counts and shapes of diverse metal clusters using a minimum of computation;

(2) the ability to generate reasonable electron-precise bonding models for metal clusters that appear intractable by other methods not requiring heavy computation;

(3) information concerning the distribution of total metal cluster electron counts between skeletal bonding within the cluster polyhedron and bonding to external ligands; and

(4) ability to distinguish between localized and delocalized bonding in metal cluster polyhedra.

Metal clusters treated effectively by this approach include post-transition element clusters [2–4], osmium carbonyl clusters [5], gold clusters [6,7], platinum carbonyl clusters [6,8], rhodium carbonyl clusters consisting of fused polyhedra [9,10], cobalt carbonyl clusters containing interstitial carbon atoms [11], nickel carbonyl clusters [12], palladium carbonyl clusters with capped polyhedra [13], metal carbonyl clusters containing alkylphosphinidene vertices [14], early transition metal halide clusters [15–17], and gallium clusters [18].

In our approach, the topology of chemical bonding can be represented by a graph in which the vertices correspond to atoms or orbitals participating in the bonding and the edges correspond to bonding relationships. The adjacency matrix, **A**, of any graph, including a graph representing chemical bonding as above, can be defined as follows:

$$A_{ij} = \begin{cases} 0 & \text{if } i = j \\ 1 & \text{if } i \text{ and } j \text{ are connected by an edge} \\ 0 & \text{if } i \text{ and } j \text{ are not connected by an edge} \end{cases} \quad (1)$$

The eigenvalues of the adjacency matrix, **A**, are obtained from the following determinantal equation:

$$|\mathbf{A} - x\mathbf{I}| = 0 \quad (2)$$

in which **I** is the unit matrix ($I_{ii} = 1$ and $I_{ij} = 0$ for $i \neq j$).

These eigenvalues, x, relate to the Hückel theory molecular orbital energies E_k for molecular orbital k and the Hückel parameters α, β, and S by the equation [1]

$$E_k = \frac{\alpha + x_k\beta}{1 + x_k S} \quad (3)$$

Positive and negative eigenvalues x_k thus correspond to bonding and antibonding orbitals, respectively.

The atoms at the vertices of metal clusters can be classified as *light atoms* or *heavy atoms*. A light atom such as boron or carbon uses only its s and p orbitals for chemical bonding and therefore has four valence orbitals (sp^3) which require eight electrons for a stable closed shell spherical bonding manifold (i.e. the Lewis octet rule). A heavy atom, such as a transition metal or post-transition metal, uses s, p, and d orbitals for chemical bonding and therefore has nine valence orbitals (sp^3d^5) which require 18 electrons for a stable closed shell spherical bonding manifold (i.e. the stable 18-electron configurations of most transition metal carbonyl derivatives). The valence orbitals of the vertex atoms are partitioned into *internal orbitals*, involved in the skeletal bonding of the cluster polygon or polyhedron, and *external orbitals*, involved in bonding to external groups or ligands such as monovalent external groups (e.g. hydrogen, halogen, alkyl, aryl) in the case of light atom vertices and carbonyl groups, tertiary phosphines, cyclopentadienyl, benzene, lone electron pairs, etc., in the case of transition metal heavy atom vertices.

The two extreme types of chemical bonding in metal clusters may be called *edge-localized* and *globally delocalized* [1,19]. An edge-localized polyhedron has two-electron two-center bonds along each edge of the polyhedron and is favored when the numbers of internal orbitals of the vertex atoms match the numbers of edges meeting at the corresponding vertices (i.e. the vertex *degree*). Since vertex atoms in metal clusters normally use three internal orbitals for cluster bonding, cluster polyhedra exhibiting pure edge-localized bonding normally have only degree three vertices, such as the tetrahedron, cube, regular dodecahedron or various prisms (Fig. 1). A globally delocalized polyhedron has a multicenter core bond in the center of the polyhedron and is formed when the numbers of internal orbitals do *not* match the vertex degrees. Intermediate degrees of delocalization may occur in sufficiently large or complicated polyhedral networks.

An important achievement of the graph-theory derived approach to the bonding topology in globally delocalized structures is the demonstration of the close analogy between the bonding in two-dimensional planar polygonal aromatic systems such as benzene and that in three-dimensional boranes and carboranes based on deltahedra

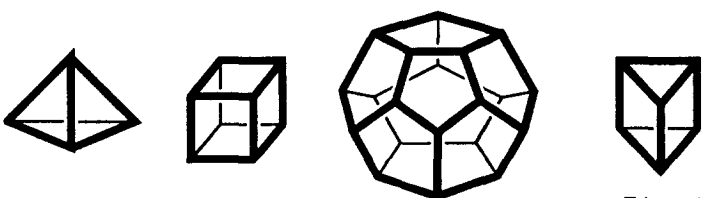

Fig. 1. Some polyhedra which have only degree 3 vertices and which therefore are suitable for edge-localized bonding in clusters of atoms using the normal three internal orbitals.

without tetrahedral chambers [1,19]. In this context, a *deltahedron* is defined to be a polyhedron in which all faces are triangles (Fig. 1). In both the two-dimensional and three-dimensional structures, the three internal orbitals from each vertex atom are partitioned into two twin internal orbitals and a single unique internal orbital. In the two-dimensional planar polygonal structures (e.g. $C_5H_5^-$, C_6H_6, $C_7H_7^+$), the twin internal orbitals overlap pairwise to form the so-called σ-bonding network around the circumference of the polygon and the unique internal orbitals overlap cyclically to form the so-called π-bonding network. In the three-dimensional deltahedral structures (e.g. $B_nH_n^{2-}$, $C_2B_{n-2}H_n$), the twin internal orbitals overlap pairwise in the surface of the polyhedron and the unique internal orbitals form a multicenter core bond at the center of the polyhedron with the overlap corresponding to a K_n complete graph in which every vertex is connected by an edge to every other vertex.

The above bonding model for globally delocalized deltahedra makes the crude but convenient assumption that all pairwise overlaps of unique internal orbitals are the same despite different pairwise relationships such as the cis and trans relationships in an octahedron or the ortho, meta, and para relationships of an icosahedron. This assumption can be evaluated by comparison of the molecular orbital energy parameters in octahedral $B_6H_6^{2-}$ obtained from this graph-theory derived model with those obtained from various computations. This comparison is the simplest in the case of the 1962 LCAO-MO extended Hückel computations of Hoffmann and Lipscomb [20]. In these computations, unlike later more sophisticated computations, the energies of pure core and surface molecular orbitals can be determined by removing the effects of mixing core and surface molecular orbitals belonging to the same irreducible representation of the O_h point group of the octahedron. This analysis [21] indicates that the energies obtained from the Hoffmann/Lipscomb computations [20] correspond to a ratio of 0.625 for the overlap of the unique internal orbitals of the trans atom pairs relative to the cis atom pairs as compared with a ratio of unity implied by an unweighted K_6 graph in the octahedral $B_6H_6^{2-}$. This level of agreement is more than sufficient for the simple graph-theory derived model to lead to the correct number of bonding orbitals and therefore the correct number of skeletal electrons. A similar comparison of the above graph-theory derived model and the Hoffmann/Lipscomb computations [20] for icosahedral $B_{12}H_{12}^{2-}$ is considerably more complicated [21] but indicates that core–surface mixing of the corresponding T_{1u} orbitals is necessary for the two methods to agree at the level of giving the same number of skeletal bonding molecular orbitals. In more recent work, similar comparisons of the graph-theory derived molecular orbital energy parameters were made using Armstrong/Perkins/Stewart self-consistent molecular orbital calculations [22] and ab initio Gaussian 82 computations [23] on $B_6H_6^{2-}$ and $B_{12}H_{12}^{2-}$. The approximation of atomic orbitals by a sum of Gaussians, as is typical in modern ab initio computations, leads to significantly weaker core bonding relative to surface bonding as well as weaker interactions between the unique internal orbitals on non-adjacent atoms (e.g. a trans pair of atoms in an octahedron or a meta or para pair of atoms

in an icosahedron) relative to adjacent atoms (e.g. a cis pair of atoms in an octahedron or an ortho pair of atoms in an icosahedron).

The general approach for considering metal cluster bonding models involves calculating the number of available skeletal electrons for comparison with the number of skeletal electrons required to fill the bonding molecular orbitals for various cluster shapes and bonding topologies. If vertex atoms furnishing the normal three internal orbitals are considered, then BH, $Fe(CO)_3$, C_5H_5Co, and Pb vertices are examples of donors of two skeletal electrons and CH, $Co(CO)_3$, C_5H_5Ni, and Bi vertices are examples of donors of three skeletal electrons. Such relationships provide isoelectronic and isolobal [24] relationships between light atom and transition metal vertices leading, for example, to long-recognized analogies [25] between polyhedral boranes and carboranes on the one hand and transition metal clusters on the other.

The globally delocalized deltahedra having n vertices (Fig. 2) have $2n+2$ skeletal electrons [26] with $2n$ of these electrons arising from the surface bonding and the remaining two electrons arising from the single bonding molecular orbital generated by the multicenter core bond [1,19]. Electron-rich polyhedra having more than $2n+2$ apparent skeletal electrons have one or more non-triangular faces (Fig. 3), whereas electron-poor deltahedra having less than $2n+2$ apparent skeletal electrons have one or more tetrahedral chambers (Fig. 4). If a deltahedron having $2n+2$ skeletal electrons is regarded as topologically homeomorphic to a sphere, then a so-called *nido* polyhedron having $2n+4$ skeletal electrons is topologically homeomorphic to a sphere with a hole in it, corresponding to the single non-triangular face.

The graph-theory derived method can also be used to derive reasonable electron-precise chemical bonding models for more complicated metal cluster structures. For example, globally delocalized rhodium octahedra can be fused by sharing triangular faces similar to the fusion of benzene rings by sharing edges (Fig. 5) [9,10]. Other rhodium carbonyl clusters have interstitial atoms which may contribute all of their valence electrons to the skeletal bonding. A prototypical example is $Rh_{13}(CO)_{24}H_2^{3-}$ (Fig. 6) in which the volume requirement of the central interstitial rhodium atom expands the outer Rh_{12} polyhedron from an icosahedron to a more voluminous cuboctahedron which, however, retains the globally delocalized bonding characteristic of icosahedral structures [9,10]. Platinum carbonyls form some unusual clusters (Fig. 7) consisting of stacked triangles (e.g. $Pt_9(CO)_{18}^{2-}$) or threaded stacked pentagons (e.g. $Pt_{19}(CO)_{22}^{4-}$) [6,8]. Electron-precise bonding models can be derived for these platinum clusters using edge-localized bonding in the platinum stack and delocalized bonding at each end of the platinum stack. The end triangles in stacked platinum triangle clusters such as $Pt_9(CO)_{18}^{2-}$ may be regarded as Möbius triangles [27] constructed from platinum d orbitals which change phase at each platinum atom [6,8]. The ends of the threaded pentagonal stack $Pt_{19}(CO)_{22}^{4-}$ may be regarded as *nido* pyramidal cavities electronically similar to the pentagonal pyramidal boron hydride B_6H_{10} [6,8].

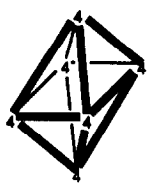

Octahedron

Pentagonal Bipyramid

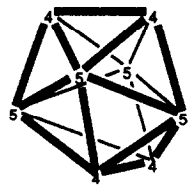

Bisdisphenoid
("D_{2d} Dodecahedron")

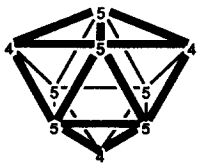

3,3,3-Tricapped Trigonal Prism

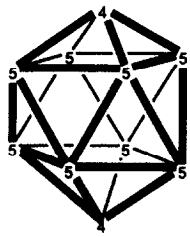

4,4-Bicapped Square Antiprism

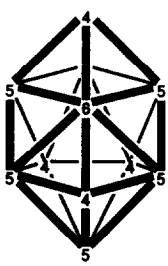

Edge-coalesced Icosahedron

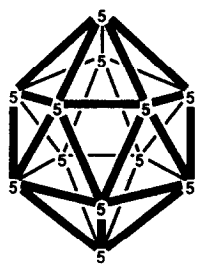

Regular Icosahedron

Fig. 2. Chemically significant deltahedra having 6–12 vertices and no tetrahedral chambers (i.e. no degree 3 vertices). The numbers on the vertices indicate their degrees (i.e. number of edges meeting at that vertex).

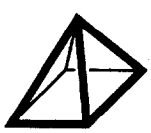

Square Pyramid

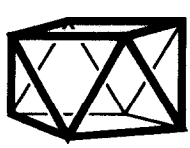

Square Antiprism

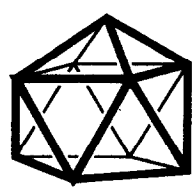

Capped Square Antiprism

Fig. 3. Some chemically significant polyhedra having one or two non-triangular faces.

Fig. 4. Examples of chemically significant polyhedra with tetrahedral chambers; all of these polyhedra are found in osmium carbonyl derivatives.

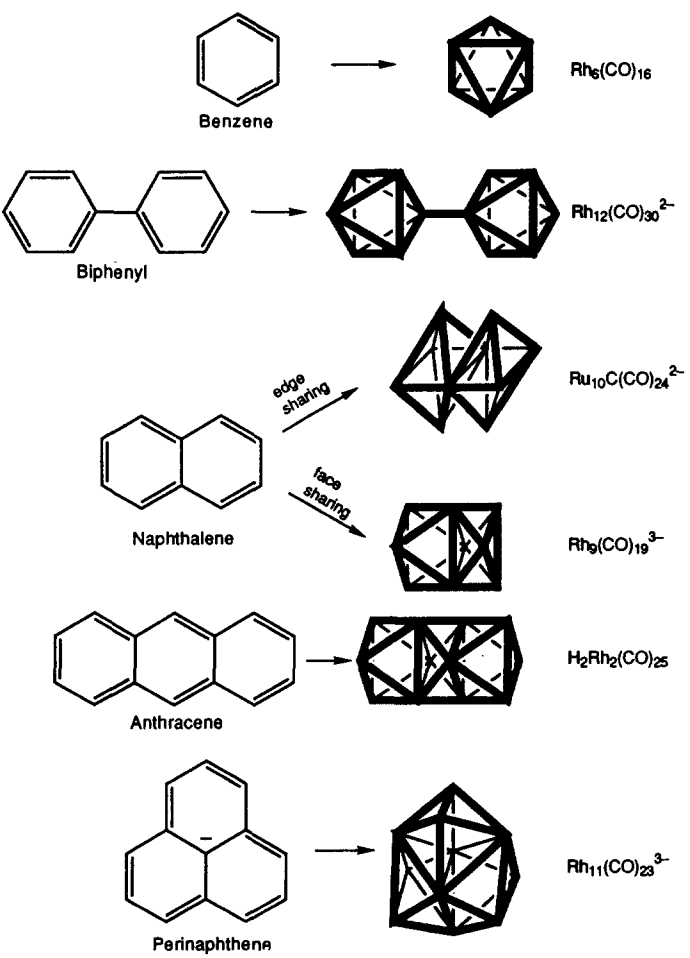

Fig. 5. Some analogies between the fusion of rhodium and ruthenium carbonyl octahedra by sharing triangular faces and the fusion of benzene rings by sharing edges.

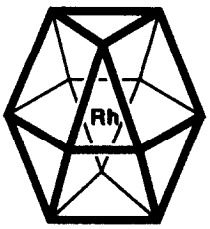

Fig. 6. The centered cuboctahedron found in $Rh_{13}(CO)_{24}H_2^{3-}$ and related clusters showing the interstitial rhodium atom in the center.

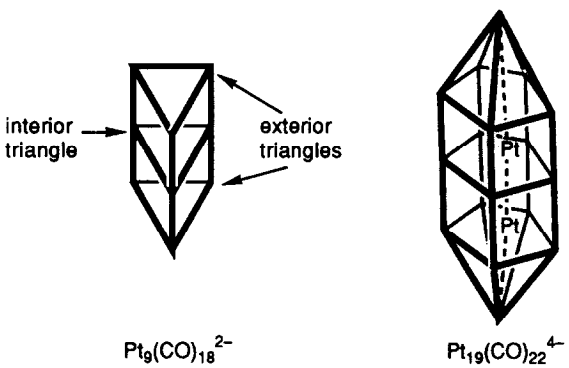

Fig. 7. Examples of stacked triangle and stacked threaded pentagon platinum carbonyl clusters. The two interstitial platinum atoms are shown in $Pt_{19}(CO)_{22}^{4-}$.

C. POLYHEDRAL ISOMERIZATIONS

The role of polyhedra in the static description of chemical structures, including those of coordination compounds and metal clusters, makes the dynamic properties of polyhedra also of considerable interest. The central concept in the study of dynamic properties of polyhedra is that of a *polyhedral isomerization*, which may be defined as the deformation of a specific polyhedron P_1 until the vertices define a new polyhedron P_2. Of particular interest are sequences of two polyhedral isomerization steps $P_1 \rightarrow P_2 \rightarrow P_3$ in which the polyhedron P_3 is equivalent to the polyhedron P_1 but with some permutation of the vertices; such a polyhedral isomerization process is called a *degenerate* polyhedral isomerization with P_2 as the *intermediate polyhedron.* A degenerate polyhedral isomerization in which the intermediate P_2 is a planar polygon may be called a *planar polyhedral isomerization.*

Polyhedral isomerizations may be treated from either the microscopic or macroscopic points of view. The microscopic view uses the details of polyhedral topology to elucidate possible single polyhedral isomerization steps. The macroscopic view presents the relationships between different polyhedral isomers as graphs called *topological representations* in which the vertices depict different permutational isomers of a given polyhedron and the edges depict single degenerate polyhedral isomerization

steps [28]. Typically, the midpoints of the edges correspond to an intermediate polyhedron.

A necessary prerequisite to understanding the dynamics of polyhedra is the static topology of polyhedra. Of basic importance are relationships between possible numbers and types of vertices (v), edges (e), and faces (f) of polyhedra. Most fundamental is Euler's relationship

$$v - e + f = 2 \tag{4}$$

The edges may be related to the faces and vertices as follows where f_i and v_j refer to the numbers of faces with i edges and vertices of degree j, respectively:

$$\sum_{i=3}^{v-1} i f_i = 2e \tag{5a}$$

$$\sum_{j=3}^{v-1} j v_j = 2e \tag{5b}$$

Since $f_i = v_i = 0$ for $i = 1$ and 2, the following inequalities must hold:

$$3f \leqslant 2e \tag{6a}$$

$$3v \leqslant 2e \tag{6b}$$

The equality holds for eqn. (6a) in the case of deltahedra and for eqn. (6b) in the case of polyhedra in which all vertices have degree 3.

In generating actual polyhedra, the operations of capping and dualization are often important. *Capping* a polyhedron P_1 consists of adding a new vertex above the center of one of its faces F_1 followed by adding edges to connect the new vertex with each vertex of F_1. This capping process gives a new polyhedron P_2 having one more vertex than P_1. If a triangular face is capped, the following relationships will be satisfied where the subscripts 1 and 2 refer to P_1 and P_2, respectively: $v_2 = v_1 + 1$; $e_2 = e_1 + 3$; $f_2 = f_1 + 2$. Such a capping of a triangular face is found in the capping of an octahedron to form a capped octahedron, i.e.:

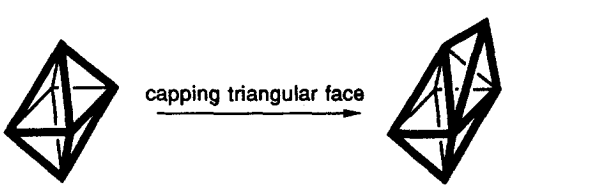

Octahedron
$v = 6, e = 12, f = 8$

Capped Octahedron
$v = 7, e = 15, f = 10$

In general, if a face with f_k edges is capped, the following relationships will be satisfied: $v_2 = v_1 + 1$; $e_2 = e_1 + f_k$; $f_2 = f_1 + f_k - 1$. An example of such a capping process converts a pentagonal pyramid into a pentagonal bipyramid by capping the pentagonal face, i.e.

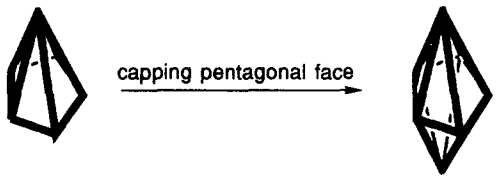

Pentagonal Pyramid
$v = 6, e = 10, f = 6$

Pentagonal Bipyramid
$v = 7, e = 15, f = 10$

A given polyhedron P can be converted into its dual P* by locating the centers of the faces of P* at the vertices of P and the vertices of P* above the centers of the faces of P. Two vertices in the dual P* are connected by an edge when the corresponding faces in P share an edge. An example of the process of dualization is the conversion of a regular octahedron to a cube, i.e.

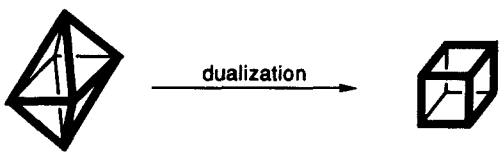

P
Octahedron
$v = 6, e = 12, f = 8$

*P**
Cube
$v = 8, e = 12, f = 6$

The process of dualization has the following properties:

(1) The numbers of vertices and edges in a pair of dual polyhedra P and P* satisfy the relationships $v^* = f$, $e^* = e$, $f^* = v$.

(2) Dual polyhedra have the same symmetry elements and thus belong to the same symmetry point group.

(3) Dualization of the dual of a polyhedron leads to the original polyhedron.

(4) The degrees of the vertices of a polyhedron correspond to the number of edges in the corresponding face polygons in its dual.

The problem of classification and enumeration of polyhedra is a complicated one. Thus there appear to be no formulae, direct or recursive, for which the number of topologically (combinatorially) distinct polyhedra having a given number of vertices, edges, faces, or any combination of these elements can be calculated [29,30]. Duijvestijn and Federico have enumerated by computer the polyhedra having up to 22 edges according to their numbers of vertices, edges, and faces and their symmetry groups and present a summary of their methods, results, and literature references to previous work [31]. Their work shows that there are 1, 2, 7, 34, 257, 2606, and 32 300 topologically distinct polyhedra having 4, 5, 6, 7, 8, 9, and 10 faces or vertices, respectively. Tabulations are available for all 301 (= 1 + 2 + 7 + 34 + 257) topologically distinct polyhedra having eight or fewer faces [32] or eight or fewer vertices [33]. These two tabulations are essentially equivalent by the dualization relationship discussed above.

Now consider some microscopic aspects of polyhedral isomerizations. As early

as 1966, Lipscomb [34] described framework rearrangements (isomerizations) in boranes and carboranes in terms of diamond-square-diamond (dsd) processes. Such a dsd process in a polyhedron occurs at two triangular faces sharing an edge and can be depicted as follows:

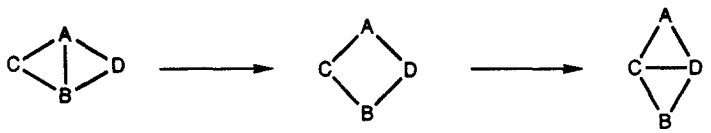

Ia **Ib** **Ic**

A configuration such as **Ia** can be called a *dsd situation*, the edge AB a *switching edge*, and the quadrilateral face ACBD in structure **Ib** a *pivot face* [35]. If *a*, *b*, *c*, and *d* are the degrees of vertices A, B, C, and D, respectively, then the requirement for a degenerate dsd process is

$$c = a - 1 \text{ and } d = b - 1 \text{ or}$$
$$c = b - 1 \text{ and } d = a - 1 \qquad (7)$$

A deltahedron with *e* edges has *e* distinct dsd situations; if at least one of these dsd situations is degenerate by satisfying eqn. (7), then the deltahedron is *inherently fluxional* [35]. If none of the *e* distinct dsd situations of a deltahedron is degenerate by satisfying eqn. (7), then the deltahedron is *inherently rigid*. The inherent rigidity/fluxionality of deltahedra having various numbers of vertices (Fig. 2) is summarized in Table 1; the chemical significance of this is summarized elsewhere [35].

Now consider some macroscopic aspects of polyhedral isomerizations as depicted by topological representations [28], which are graphs in which the vertices correspond to isomers and the edges correspond to isomerization steps. For isomerizations of a polyhedron having *n* vertices, the number of vertices in the topological

TABLE 1
Inherent rigidity/fluxionality of deltahedra

Vertices	Deltahedron (Fig. 1)	Inherently rigid or fluxional
4	Tetrahedron (T_d)	Rigid
5	Trigonal bipyramid (C_{3v})	Fluxional
6	Octahedron (O_h)	Rigid
7	Pentagonal bipyramid (D_{5h})/capped octahedron (C_{3v})	ML_7→fluxional Boranes→rigid
8	Bisdisphenoid (D_{2d}) ("D_{2d} dodecahedron")	Fluxional
9	Tricapped trigonal prism (D_{3h})	Fluxional
10	Bicapped square antiprism (D_{4d})	Rigid
11	Edge-coalesced icosahedron (C_{2v})	Fluxional
12	Icosahedron (I_h)	Rigid

representation is the isomer count I where

$$I = \frac{n!}{|R|} \tag{8}$$

and $|R|$ is the number of proper rotations (E plus all C_ks) in the symmetry point group of the polyhedron in question. The degree of a vertex corresponds to the number of distinct permutational isomers which can be generated in a single isomerization step from the isomer represented by the vertex in question; this number, δ, is called the *connectivity*. For topologically distinct polyhedra depicted in the same topological representation, the isomer counts I and I' and connectivities δ and δ' must satisfy the so-called closure condition [28], i.e.

$$I\delta = I'\delta' \tag{9}$$

A simple illustration of these ideas is provided in the four-vertex system by the topological representation of the degenerate planar isomerization of a tetrahedron into its enantiomer through a square planar intermediate (Fig. 8) [28]. The isomer count for the tetrahedron, I_{tet}, is $4!/|T| = 24/12 = 2$ and the isomer count for the

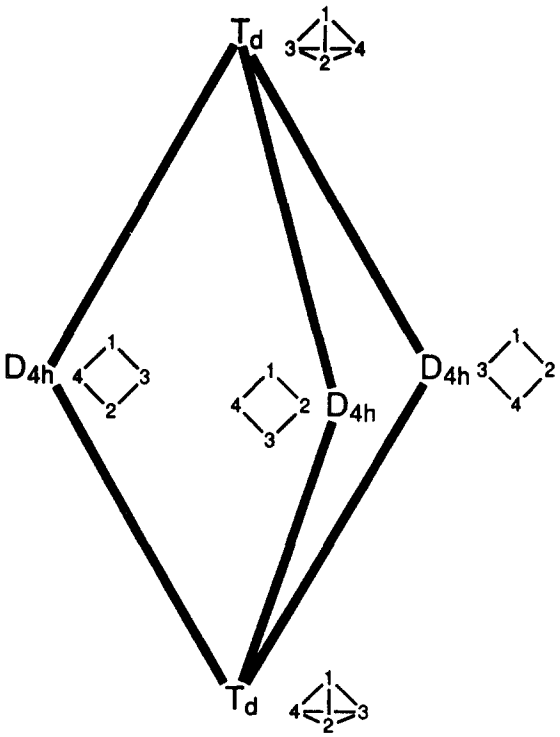

Fig. 8. The $K_{2,3}$ bipartite graph as a topological representation of the degenerate planar isomerization of a tetrahedron (T_d) into its enantiomer through a square planar intermediate (D_{4h}). The isomers corresponding to the vertices of the $K_{2,3}$ bipartite graph are depicted next to the vertex labels.

square, I_{sq}, is $4!/|D_4| = 24/8 = 3$. A topological representation for this process is a $K_{2,3}$ bipartite graph which is derived from the trigonal bipyramid by deletion of the three equatorial–equatorial edges (Fig. 8). The two axial vertices correspond to the two tetrahedral isomers and the three equatorial vertices correspond to the three square planar isomers. The connectivities of the tetrahedral (δ_{tet}) and square planar (δ_{sq}) isomers are 3 and 2, respectively, in accord with the degrees of the corresponding vertices of the $K_{2,3}$ graph (Fig. 8). Since $I_{tet}\delta_{tet} = I_{sq}\delta_{sq} = 6$, the closure condition (eqn. (9)) is satisfied for this topological representation.

The topological representations of isomerizations of polyhedra having five or more vertices lead to some interesting graphs [28]. The 20-vertex Desargues–Levy graph (Fig. 9, top) is a topological representation of isomerizations of the 20 trigonal bipyramid permutation isomers through the 30 square pyramid permutation isomer

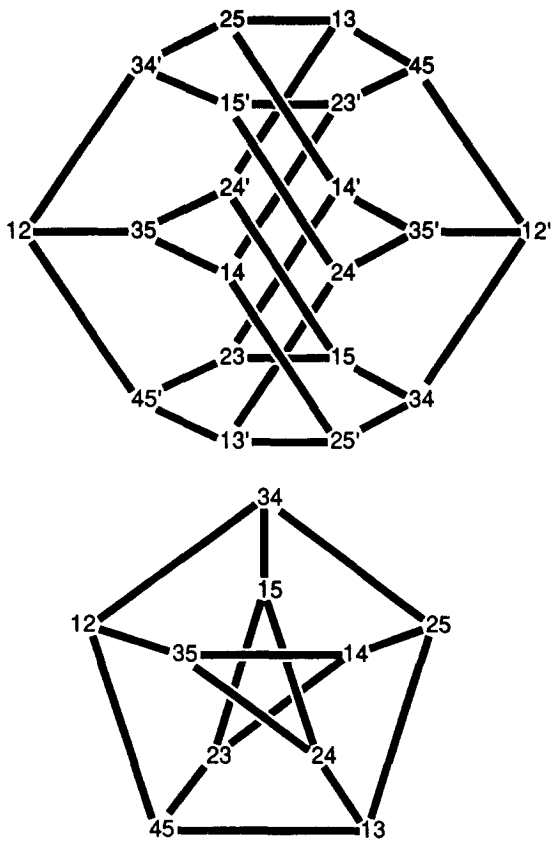

Fig. 9. Topological representations of the isomerizations of trigonal bipyramids through dsd processes (Berry pseudorotations). The two digits represent labels for the axial positions with primes used to indicate enantiomers. Top: Desargues–Levy graph as a topological representation for dsd isomerizations of the 20 trigonal bipyramid isomers. Bottom: The Petersen graph as a topological representation for dsd isomerizations of the 10 enantiomer pairs of the trigonal bipyramid isomers.

intermediates represented by the edge midpoints; these isomerizations correspond to Berry pseudorotations in five-coordinate complexes [36,37]. If the 20 trigonal bipyramid permutation isomers are depicted as the corresponding 10 pairs of enantiomers, then the topological representation reduces to the Petersen's graph (Fig. 9, bottom), which is of interest since it has both three-fold and five-fold symmetry. A topological representation of six-vertex polyhedral isomerizations is a double group regular dodecahedron with a K_5 complete graph (i.e. a pentagon and a pentagram with all five vertices in common) in each of the 12 faces (Fig. 10). The 30 edge midpoints of the dodecahedron (spades, ♠, in Fig. 10) correspond to the 30 octahedron permutation isomers and the (12)(10) = 120 edge midpoints of the 12 K_5 graphs on the dodecahedron faces (diamonds, ♦, in Fig. 10) correspond to the 120 trigonal prism intermediates in trigonal twist [28,38] (i.e. Bailar twist or Ray and Dutt twist triple dsd processes).

In the cases of isomerizations of polyhedra having more than six vertices, the isomer counts (eqn. (8)) are too large (e.g. $I_{\text{cube}} = 8!/|O| = 40\,320/24 = 1680$) for topological representations to be depicted graphically in a tractable manner. In the case of eight-vertex polyhedra, a tractable graphical topological representation can be obtained by "hyperoctahedral restriction" since the 384-operation symmetry group of the four-dimensional cube or tesseract (Fig. 11) contains the symmetries of all of the eight-vertex polyhedra of actual or potential chemical significance, including the ordinary cube as well as the hexagonal bipyramid, square antiprism, and bisdisphenoid ("D_{2d} dodecahedron") [39]. The hyperoctahedrally restricted isomerizations of these four eight-vertex polyhedra can be depicted by the topological representation in Fig. 12, namely a $K_{4,4}$ bipartite graph having eight hexagon vertices [39]. The

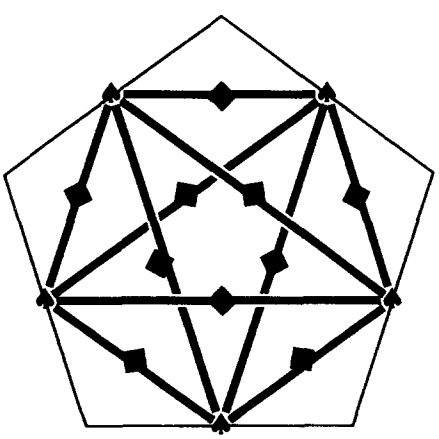

Fig. 10. One of the twelve pentagonal faces of the I_h double group (pentagonal dodecahedron) used as a topological representation for the degenerate triple dsd isomerization of the octahedron (O_h) through a trigonal prismatic intermediate (D_{3h}). The five spades (♠) at the midpoints of the sides of the face represent five of the 30 octahedron permutational isomers whereas the 10 diamonds (♦) at the midpoints of the edges of the K_5 graph drawn on the face represent 10 of the 120 trigonal prism permutational isomers.

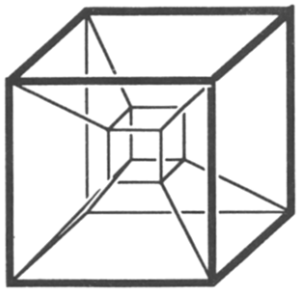

Fig. 11. The tesseract or "four-dimensional cube" projected into two dimensions.

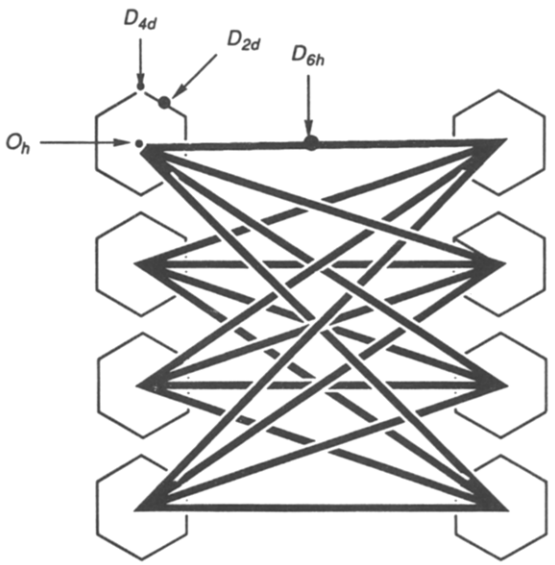

Fig. 12. The $K_{4,4}$ bipartite graph of hexagons in a hyperoctahedrally restricted topological representation of isomerizations of eight-vertex polyhedra showing the locations of one of the eight cubes (O_h), 16 hexagonal bipyramids (D_{6h}), 48 square antiprisms (D_{4d}), and 48 bisdisphenoids (D_{2d}).

midpoints of the 16 edges of the $K_{4,4}$ bipartite graph represent hexagonal bipyramid (D_{6h}) enantiomer pairs, the eight centers of the eight hexagons represent cube (O_h) enantiomer pairs, the 48 vertices of the eight hexagons represent square antiprism (D_{4d}) enantiomer pairs, and the midpoints of the 48 edges of the eight hexagons represent bisdisphenoid (D_{2d}) enantiomer pairs. Note that when considering polyhedra for eight-coordination, sp^3d^4 hybrids suffice to form square antiprisms (Fig. 3) and bisdisphenoids (Fig. 2), which do not have an inversion center, *i*. However, hybrids containing *f* orbitals are required to form cubes and hexagonal bipyramids, which have inversion centers [40]. Thus eight-vertex isomerizations involving only s, p, and d orbitals are restricted to the perimeter of a single hexagon where square antiprism and bisdisphenoid isomers are located whereas the availability of f orbitals

as well as s, p, and d orbitals makes accessible the hexagon centers representing cubes as well as transitions between hexagons along the edges of the $K_{4,4}$ bipartite graph representing hexagonal bipyramids.

D. CONCLUSION

This article illustrates how mathematical ideas taken from disciplines such as topology and graph theory can provide a fundamental theoretical insight into key areas of coordination chemistry such as structure and bonding of metal clusters as well as polyhedral isomerizations. Such theoretical insight is most valuable in the planning of effective and efficient experimental programs in diverse areas of coordination chemistry, including work of potential practical importance relating to topics such as molecular catalysis, properties of solid state materials, and bioinorganic chemistry.

REFERENCES

1 R.B. King and D.H. Rouvray, J. Am. Chem. Soc., 99 (1977) 7834.
2 R.B. King, Inorg. Chim. Acta, 57 (1982) 79.
3 R.B. King, in P. Jena, B.K. Rao and S.N. Khanna (Eds.), The Physics and Chemistry of Small Clusters, Plenum Press, New York, 1987, pp. 79–82.
4 R.B. King, J. Phys. Chem., 92 (1988) 4452.
5 R.B. King, Inorg. Chim. Acta, 116 (1986) 99.
6 R.B. King, in N. Trinajstić (Ed.), Mathematics and Computational Concepts in Chemistry, Ellis Horwood, Chichester, 1986, pp. 146–154.
7 R.B. King, Inorg. Chim. Acta, 116 (1986) 109.
8 R.B. King, Inorg. Chim. Acta, 116 (1986) 119.
9 R.B. King, Int. J. Quantum Chem. Quantum Chem. Symp., 20 (1986) 227.
10 R.B. King, Inorg. Chim. Acta, 116 (1986) 125.
11 R.B. King, New J. Chem., 12 (1988) 493.
12 R.B. King, Rev. Roum. Chim., 36 (1991) 353.
13 R.B. King, Gazz. Chim. Ital., in press.
14 R.B. King, New J. Chem., 13 (1989) 293.
15 R.B. King, in R.B. King and D.H. Rouvray (Eds.), Graph Theory and Topology in Chemistry, Elsevier, Amsterdam, 1987, pp. 325–343.
16 R.B. King, Inorg. Chim. Acta, 129 (1987) 91.
17 R.B. King, Rep. Mol. Theory, 1 (1990) 141.
18 R.B. King, Inorg. Chem., 28 (1989) 2796.
19 R.B. King, in R.B. King (Ed.), Chemical Applications of Topology and Graph Theory, Elsevier, Amsterdam, 1983, pp. 99–123.
20 R. Hoffmann and W.N. Lipscomb, J. Chem. Phys., 36 (1962) 2179.
21 R.B. King, J. Comput. Chem., 8 (1987) 341.
22 R.B. King, Inorg. Chem., 27 (1988) 1941.
23 R.B. King, B. Dai and B.M. Gimarc, Inorg. Chim. Acta, 167 (1990) 213.
24 R. Hoffmann, Angew. Chem. Int. Ed. Engl., 21 (1982) 711.
25 K. Wade, Chem. Commun., (1971) 792.

26 D.M.P. Mingos, Acc. Chem. Res., 17 (1984) 311.
27 H.E. Zimmermann, Acc. Chem. Res., 4 (1971) 272.
28 E.L. Muetterties, J. Am. Chem. Soc., 91 (1969) 1636.
29 F. Harary and E.M. Palmer, Graphical Enumeration, Academic Press, New York, 1973, p. 224.
30 W.T. Tutte, J. Combin. Theory Ser. B, 28 (1980) 105.
31 A.J.W. Duijvestijn and P.J. Federico, Math. Comput., 37 (1981) 523.
32 P.J. Federico, Geom. Ded., 3 (1975) 469.
33 D. Britton and J.D. Dunitz, Acta Crystallogr. Sect. A, 29 (1973) 362.
34 W.N. Lipscomb, Science, 153 (1966) 373.
35 R.B. King, Inorg. Chim. Acta, 49 (1981) 237.
36 R.S. Berry, J. Chem. Phys., 32 (1960) 933.
37 R.R. Holmes, Acc. Chem. Res., 5 (1972) 296.
38 E.L. Muetterties, J. Am. Chem. Soc., 90 (1968) 5097.
39 R.B. King, Theor. Chim. Acta, 59 (1981) 25.
40 R.B. King, Theor. Chim. Acta, 64 (1984) 453.